The statistics of noisy growth with mechanical feedback in elastic tissues

Ojan Khatib Damavandi[a,1] **and David K. Lubensky**[a,2]

[a]Department of Physics, University of Michigan, Ann Arbor MI, USA 48109

This manuscript was compiled on September 24, 2018

Tissue growth is a fundamental aspect of development and is intrinsically noisy. Stochasticity has important implications for morphogenesis, precise control of organ size, and regulation of tissue composition and heterogeneity. Yet, the basic statistical properties of growing tissues, particularly when growth induces mechanical stresses that can in turn affect growth rates, have received little attention. Here, we study the simple case of noisy growth of elastic sheets subject to mechanical feedback. Considering both isotropic and anisotropic growth, we find that the density-density correlation function shows power law scaling. We also consider the dynamics of marked clones of cells. We find that the areas (but not the shapes) of two clones are always statistically independent, even when they are adjacent. For anisotropic growth, we show that clone size variance scales like the average area squared and that the mode amplitudes characterizing clone shape show a slow $1/n$ decay, where n is the mode index. This is in stark contrast to the isotropic case, where relative variations in clone size and shape vanish at long times. The high variability in clone statistics observed in anisotropic growth is due to the presence of two soft modes — growth modes that generate no stress. Our results lay the groundwork for more in-depth explorations of the properties of noisy tissue growth in specific biological contexts.

tissue mechanics | noisy growth | clonal dynamics | fluctuations | mechanical feedback

Growth is central to biology and usually involves a level of stochasticity (1–3). The presence of such noise can have significant consequences for developmental processes like morphogenesis and the regulation of organ size. Yet, little is known about quantitative aspects of stochastic growth, especially in elastic tissues where mechanical feedback is expected. Our goal here is to understand the interplay between noise and mechanical feedback in growing elastic tissues. To that end, we present a generic, continuum model of such tissues and use it to study measurable features of tissue architecture like density fluctuations and statistics of marked clones. This model makes a number of unexpected predictions, including the presence of power law correlations in space and the existence of soft modes that allow clone sizes to grow diffusively, evading the effects of mechanical feedbacks that might otherwise be expected to limit clone size variability.

In experiments, noise in growth has most often been probed through the size and spatial distribution of clones of cells (4–10). Cell density variation has also been observed directly in culture systems (11–15) and in fixed tissues (16), and size asymmetry between two contralateral organs can be used as an indirect readout of noise levels (17). Theoretically, the most thoroughly explored area is the noisy dynamics of stem cell populations (4, 5, 9), where zero-dimensional descriptions are often appropriate and spatial crowding effects, when important, have been included at the level of simple lattice models. Similar models apply to fluid tissues where clone fragmentation and aggregation is the dominant process at long times (6). Here, in contrast, our goal is to explicitly include the effects of mechanical stresses on growth. In particular, we expect that noise will lead to growth non-uniformities and thus to the uneven accumulation of cell mass; this, in turn, will generate stresses that can feed back on local growth rates. Such effects are taken into account in a related study by Ranft et al. (18), who show that mechanical feedbacks cause the stress tensor to relax as if the tissue were a viscoelastic fluid; their treatment of noise, however, is limited to fluctuations about zero average growth, where most of the phenomena of interest here are absent.

On a very basic level, the idea of mechanical feedback on tissue growth is uncontroversial—cells obviously cannot grow indefinitely into space occupied by other cells, so some sort of contact inhibition or crowding effects must be present. Whether cells more generally adjust their growth rates to their mechanical environment is, however, less obvious. The idea that negative feedback from mechanical stresses could damp out cell density fluctuations was proposed in (19) and has since been incorporated into a number of models (8, 20–31). On the experimental front, examples of mechanical feedback in living animals have been more difficult to obtain (32, 33). Nonetheless, several studies have argued that tissues both in culture (12, 34–36) and *in vivo* (37–39) respond to mechanical stress by modulating the rate and orientation of cell division or by inducing cell death (36, 40–42). Clones of fast-growing cells in *Drosophila* wing imaginal discs reduce their growth rate through mechanical feedback (8). Similar behavior has been observed in the *Arabidopsis* sepal (10), and other studies have shown further evidence for mechanical feedback in plants (29, 43). In confluent monolayers, contact inhibition leads to reduced mitotic rates (11, 15). Finally, cell aggregates (44–47) and bacterial populations (48) also appear to respond to mechanical cues. Thus, even if the evidence is not yet completely conclusive, it seems likely that some mechanical feedback on growth is present in many tissues.

In what follows, we first introduce our basic framework, which assumes linear elastic deformations about a uniformly growing reference state and linear feedback of the stress tensor on the local growth rate. We then consider the special case of isotropic growth, where we show that density-density correlations generically decay with distance as a power law and that mechanical feedback effectively drives clone size variability to zero on large scales. We also find that the areas of neighboring clones are statistically uncorrelated. We then

O.K.D. and D.K.L. performed research; and O.K.D. and D.K.L. wrote the paper.

The authors declare no conflict of interest.

[1]Email: ojan@umich.edu [2]Email: dkluben@umich.edu

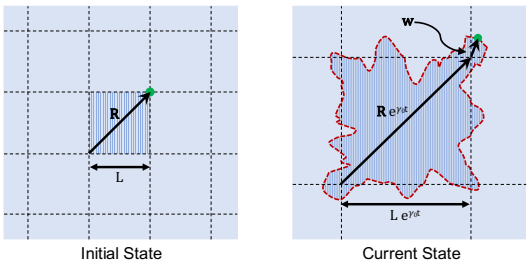

Fig. 1. Noisy growth leads to tissue deformation. A shaded square of length L in the initial state is transformed after noisy growth for time t into a region with deformed boundaries (red) in the current state. The displacement of a point (green dot) at the corner of the shaded square is also shown. This point is displaced to $\mathbf{R}e^{\gamma_0 t} + \mathbf{w}$ after time t. Dashed grid lines visualize the uniform average tissue dilation.

turn to the more general case of anisotropic growth. Here, we observe the appearance of soft modes, where faster than average growth of one tissue region is exactly compensated by slower growth in surrounding regions and elastic deformations so as to leave the tissue completely stress-free; these modes can thus grow without bound even in the presence of feedback. As a consequence, clone sizes display a standard deviation of order their mean, in strong contrast to the isotropic case.

Basic Model

We consider a flat epithelium undergoing isotropic, exponential growth on average, with small, random deviations from this average. Although many of our results can be straightforwardly generalized to higher dimensions, we limit ourselves here to two-dimensional tissues. At the macroscopic scale, we can view the epithelium as a continuum elastic material. Growth then looks like local creation of mass, and non-uniform growth can in turn induce tissue deformations. We focus on the simplest case of an infinite tissue and thus ignore boundary effects.

With these assumptions, we define two coordinate systems: the reference (Lagrangian) system $\{\mathbf{R}\}$ and the material (Eulerian) system $\{\mathbf{r}\}$ describing the system's current, deformed state. Each point on the tissue at time t is related to a point in the reference coordinates by $\mathbf{r} = \mathrm{e}^{\gamma_0 t}\mathbf{R} + \mathbf{w}$, where γ_0 is the average growth rate and $\mathbf{w}$ is the local deformation due to growth fluctuations (Fig. 1).

Growth is represented by the symmetric second rank tensor $\mathrm{G}(\mathbf{R})$ (see, e.g., (49)). Its principal components give the tissue's preferred dilation—that is, the factor by which the tissue particle at $\mathbf{R}$ must expand to remain stress free—along the two principal axes. It can be decomposed as $\mathrm{G}(\mathbf{R}) = \bar{G}\mathbb{1} + \widetilde{\mathrm{G}}(\mathbf{R})$, where the scalar $\bar{G} = \mathrm{e}^{\gamma_0 t}$ describes the spatially uniform, average tissue expansion, and the tensor $\widetilde{\mathrm{G}}(\mathbf{r})$ represents fluctuations about the average.

We assume that growth is slow enough that the tissue is always at mechanical equilibrium; absent any external forces or confinement, spatially uniform growth should then not generate any mechanical stress, which will instead be caused entirely by the spatially-varying component $\widetilde{\mathrm{G}}$ of the growth tensor. In the limit of weak fluctuations in growth rate, $\widetilde{\mathrm{G}}$ and $\mathbf{w}$ will both be small, and we can linearize at each instant about the uniformly dilated state. The resulting description of tissue elasticity has a form familiar from the theory of thermoelasticity (50, 51). We define a strain-like tensor $w_{ij} = (\partial_i w_j + \partial_j w_i)/2$, where ∂_i denotes the partial derivative with respect to R_i. (Throughout this paper, all spatial derivatives are taken with respect to Lagrangian coordinates unless otherwise specified.) The Cauchy stress tensor is then:

$$\sigma_{ij} = \frac{1}{\bar{G}}[\lambda(w_{ll} - \widetilde{G}_{ll})\delta_{ij} + 2\mu(w_{ij} - \widetilde{G}_{ij})], \qquad [1]$$

where λ and μ are the Lamé coefficients and summation on repeated indices is implied. In two dimensions, $\lambda + \mu$ is the bulk modulus. Intuitively, Eq. 1 says that the stress vanishes when the actual strain w_{ij} matches the preferred local deformation due to growth $\widetilde{G}_{ij}$ and otherwise grows linearly with the difference between these two quantities. It differs from textbook thermoelastic results only in the factor of $1/\bar{G}$, which arises from the conversion of derivatives with respect to $\mathbf{R}$ to derivatives with respect to the uniformly dilated reference coordinates $\bar{G}\mathbf{R}$. Eq. 1 can also be derived by starting from a fully nonlinear theory of morphoelasticity (49) and linearizing about uniform growth (see Supporting Information [SI]).

Given Eq. 1, force balance $\partial_i \sigma_{ij} = 0$ implies

$$(\lambda + 2\mu)\nabla(\nabla.\mathbf{w}) - \mu(\nabla \times \nabla \times \mathbf{w}) = \lambda\nabla\widetilde{G}_{ll} + 2\mu\nabla.\widetilde{\mathrm{G}}. \qquad [2]$$

This equation may be solved to obtain $\mathbf{w}$, and thus w_{ij} and σ_{ij}, at each instant as a function of $\widetilde{\mathrm{G}}$.

To complete our description of growth, we must specify the dynamics of G, whose most general possible form is

$$\partial_t \mathrm{G} = \Gamma \mathrm{G}, \qquad [3]$$

where Γ is in general a rank four tensor that incorporates mechanical feedback and noise (see SI). Throughout this text, we define ∂_t to be a time derivative taken at fixed Lagrangian coordinates $\mathbf{R}$. (The SI discusses how $\partial_t \mathrm{G}$ with this convention is related to different proposed expressions for the time derivative at fixed Eulerian coordinates.)

Assuming that deviations from uniform growth are small, we can expand Eq. 3 to linear order in stress feedbacks and noise. The most general form allowed by symmetry is

$$\partial_t \left[\frac{\widetilde{G}_{ij}}{\bar{G}}\right] = c\,\sigma_{ll}\,\frac{\delta_{ij}}{2} + c^{(d)}\left(\sigma_{ij} - \sigma_{ll}\,\frac{\delta_{ij}}{2}\right) + \xi_{ij}(\mathbf{R}, t), \qquad [4]$$

where we have also dropped higher order gradient terms (whose effects are addressed in the SI). Here the constants c and $c^{(d)}$ give the strengths of the stress feedbacks (and the superscript d stands for deviatoric).

Density. Within the framework of continuum elasticity, it is natural to define a density $\rho(\mathbf{R}, t)$ of the deformed material. For a complex biological tissue, ρ of course does not represent the total mass density but instead can be thought of as roughly the density of materials (like cytoskeletal proteins) that give the tissue an elastic rigidity or, equivalently, as a measure of elastic tissue compression or expansion relative to an ideal, unstressed state. If we call the (uniform) density in the stress free configuration ρ_0 and deviations from this density because of growth fluctuations $\delta\rho(\mathbf{R}, t) = \rho(\mathbf{R}, t) - \rho_0$, then to linear order in fluctuations,

$$\delta\rho = \frac{\rho_0}{\bar{G}}(\widetilde{G}_{ll} - w_{ll}). \qquad [5]$$

If all cells in the tissue had the same preferred apical area, then ρ would be proportional to the cell density. Even if that

is not the case, as long as cells' relaxed areas are uncorrelated, the difference between the cell density and the average of ρ over a region of area A will decrease as $1/\sqrt{A}$, allowing the cell density to be used to estimate ρ on long enough scales.

Isotropic Growth

In order to build intuition, we first consider the simplest case of isotropic growth. We thus set $\widetilde{G}_{ij} = \widetilde{G}\ \delta_{ij}$ and restrict the stress feedback and noise in Eq. 4 to be isotropic, i.e., we will only have feedback from the pressure p (in 2D, $\sigma_{ll} = -2p$).

As outlined above, we can use force balance (Eq. 2) to find w_{ij} in terms of $\widetilde{G}$. After Fourier transforming with the convention $f(\mathbf{Q},t) = \int \mathrm{d}\mathbf{R}\ e^{-i\mathbf{Q}.\mathbf{R}} f(\mathbf{R},t)$, we have $(\lambda+2\mu)(\mathbf{Q}.\mathbf{w})\mathbf{Q} - \mu(\mathbf{Q}\times\mathbf{Q}\times\mathbf{w}) = -2i(\lambda+\mu)\widetilde{G}\,\mathbf{Q}$. Solving for $\mathbf{w}$ and using Eq. 5 to relate $\delta\rho$ and $\widetilde{G}$, it is straightforward to see that

$$\mathbf{w} = -2i\frac{(\lambda+\mu)\ \mathbf{Q}}{(\lambda+2\mu)Q^2}\widetilde{G} \quad \text{and} \quad \delta\rho = \rho_0\frac{2\mu}{\lambda+2\mu}\ \frac{\widetilde{G}}{\bar{G}}.$$

Then Eq. 4 can be rewritten as

$$\partial_t\,\delta\rho(\mathbf{R},t) = -k\,\delta\rho + \rho_0\ \frac{\mu}{\lambda+2\mu}\xi(\mathbf{R},t). \qquad [6]$$

Here, $k = 2\mu(\lambda+\mu)c/(\lambda+2\mu)$, and the (scalar) noise $\xi(\mathbf{R},t)$ is delta correlated in time and spatially correlated on a length scale $a/\sqrt{2}$ of order a typical cell radius; this small but non-zero correlation length is needed to prevent pathological behavior and makes physical sense as cell growth and division is correlated on the scale of a single cell. Because cell sizes remain constant as the tissue grows, the correlation length should be viewed as fixed in Eulerian coordinates, so that $\langle\xi(\mathbf{r},t)\xi(\mathbf{r}',t')\rangle = De^{-\frac{(\mathbf{r}-\mathbf{r}')^2}{a^2}}\delta(t-t')/\pi a^2$ where D is the noise strength. In Lagrangian coordinates, the correlation function then becomes $\langle\xi(\mathbf{R},t)\xi(\mathbf{R}',t')\rangle = De^{-\frac{\bar{G}(t)^2(\mathbf{R}-\mathbf{R}')^2}{a^2}}\delta(t-t')/\pi a^2$, where we used, to leading order, $\mathbf{r}\approx\bar{G}\mathbf{R}$.

Density-density Correlations. From Eq. 6 we can calculate the density-density correlation functions, which are experimentally accessible (13, 14, 16). We find that the density-density spatial correlation function goes like a power law in steady state (formally, $t\to\infty$) and for large separations $|r-r'|\gg a$:

$$\frac{1}{\rho_0^2}\,\langle\delta\rho(\mathbf{r},t)\delta\rho(\mathbf{0},t)\rangle_{t\to\infty} \sim \left(\frac{r}{a}\right)^{\frac{-2k}{\gamma_0}}, \qquad [7]$$

where the pre-factor to the power law is $\mathcal{O}(k/\gamma_0)$ (see SI). Fig. S1 plots the full correlation function versus r/a.

To understand this behavior, suppose that random noise generates a density fluctuation correlated on a length scale a. Over time, growth will advect this fluctuation outwards while mechanical feedback will cause its amplitude to decay. After time t, the initial, small-scale fluctuation will induce correlations on a length scale $r\sim a\ e^{\gamma_0 t}$, but the magnitude of the correlations will have decayed like e^{-2kt}. For a given r, fluctuations that happened around $t^*(r) = \log(r/a)^{1/\gamma_0}$ ago are dominant; earlier fluctuations have decayed out while later ones have not reached the distance r yet. Thus, we expect $\langle\delta\rho(\mathbf{r})\delta\rho(\mathbf{0})\rangle \sim \exp[-2kt^*(r)] \sim (r/a)^{-2k/\gamma_0}$. A similar mechanism produces power law correlations in inflationary models of the early universe (52). This result requires a small but finite initial correlation length for fluctuations. Here, we assumed this lengthscale comes from the noise spectrum. The SI shows, however, that the same behavior occurs if the lengthscale is instead generated by the inclusion of gradient terms in the growth dynamics, Eq. 4 and that similar power law scaling is seen in any spatial dimension.

Finally, we look at correlation between a point initially at $\mathbf{R}$ and itself at a later time τ. This means that in Eulerian coordinates, we are looking at two different points, i.e. $(\mathbf{r},t)$ and $(\mathbf{r}',t+\tau)$, such that both points originate from $(\mathbf{R},0)$. We find that this correlator decays exponentially in time as expected from the negative feedback:

$$\frac{1}{\rho_0^2}\,\langle\delta\rho(\mathbf{R},t)\delta\rho(\mathbf{R},t+\tau)\rangle_{t\to\infty} \sim e^{-k\tau}. \qquad [8]$$

Clone Statistics. Following marked clones has proven to be a useful tool to track the time course of growth and development (4–6, 9). Here, inspired by the biological relevance and relative feasibility of studying clone dynamics (7, 8, 10), we look at the size distribution and shape statistics of clones in a growing tissue. We start from a circular clone at the center of the tissue and derive expressions for the variance of the clone area as well as the variance of mode amplitudes characterizing the clone shape.

The area of a clone with initial radius R_c is $A(t) = \int_{R\le R_c}|\partial\mathbf{r}/\partial\mathbf{R}|\,\mathrm{d}\mathbf{R} \approx \pi(\bar{G}R_c)^2 + \bar{G}\int_{R\le R_c}\nabla.\mathbf{w}\,\mathrm{d}\mathbf{R}$, to leading order in small w. The variance of clone size is then

$$\mathrm{Var}(A) = \bar{G}^2\int_{R,R'\le R_c}\langle\nabla.\mathbf{w}\ \nabla'.\mathbf{w}'\rangle\ \mathrm{d}\mathbf{R}\mathrm{d}\mathbf{R}', \qquad [9]$$

where $\nabla' = \nabla_{\mathbf{R}'}$ is the gradient operator taken with respect to $\mathbf{R}'$. To study clone shape, we describe the instantaneous clone boundary as a curve $r_c(\theta)$ in Eulerian coordinates, where θ is the polar angle, which we can then express as a Fourier series $r_c(\theta) = \sum B_n e^{in\theta}$. To linear order in $\mathbf{w}$, we may neglect differences between the Lagrangian and Eulerian polar angles Θ and θ, and $r_c = \bar{G}R_c + \hat{\mathbf{R}}.\mathbf{w}$, where $\hat{\mathbf{R}}$ is a unit vector in the direction of $\mathbf{R}$. Continuing to work to the same order, it is easy to see that

$$\left\langle|B_n|^2\right\rangle = \int_0^{2\pi}\frac{\mathrm{d}\Theta\mathrm{d}\Theta'}{(2\pi)^2}\hat{R}_k(\Theta)\hat{R}_j(\Theta')\langle w_k w_j'\rangle e^{-in(\Theta-\Theta')}, \qquad [10]$$

where $w_j' = w_j(R_c,\Theta')$.

For isotropic growth, both $\mathbf{w}$ and $\nabla.\mathbf{w}$ can be written in terms of $\delta\rho$, so Eq. 6 is all we need to solve Eqs. 9 and 10. The difference between this calculation and the density-density correlation function is that here we look at fixed Lagrangian instead of Eulerian coordinates. We find that in the isotropic case, clone size and shape variances vanish at long times relative to the dilation, i.e. $\lim_{t\to\infty}\mathrm{Var}(A)/\langle A\rangle^2 \to 0$ and $\lim_{t\to\infty}\left\langle|B_n|^2\right\rangle/B_0^2 \to 0$. This suggests that all old clones are statistically the same. In the next section, we look at more general anisotropic growth, where clone size and shape statistics show very different behaviors.

Before doing so, it is instructive to note that the areas of two adjacent clones in our model are uncorrelated, i.e. for two clones with areas A_1 and A_2, $\langle\Delta A_1\Delta A_2\rangle = 0$, where ΔA is the difference between the actual clone area and its mean

value. This is a direct consequence of the elastic response of an infinite tissue to localized growth: With $\widetilde{G} \sim \delta(\mathbf{R})$, $\mathbf{w} \sim \hat{\mathbf{r}}/r$, and $\nabla.\mathbf{w} = 0$ except at the origin. Thus, while the shapes of clones near the origin are distorted by growth, only clones that actually contain the origin change their area (Fig. 2A). Thus, the size of each clone depends only on $\widetilde{G}$ within its own boundaries, and as $\widetilde{G}$ is spatially uncorrelated beyond the size of a single cell, clone areas are also uncorrelated. This result holds for both isotropic and anisotropic growth (see SI).

Anisotropic Growth

Cells in both animal (35, 37, 38) and plant (43) tissues have been shown to orient their divisions relative to the principal axis of an applied stress. Thus, in general, we should consider stress-dependent anisotropic growth. This means that $\widetilde{\mathrm{G}}$, a symmetric two dimensional matrix, now is specified by three scalars: the trace and two components for the traceless part. We follow the same steps as in the isotropic case to solve Eq. 4 and find expressions for density-density correlators and clone statistics. We will see that density-density correlators follow a similar power law behavior as Eq. 7, but that new soft modes appear which cause clone size and shape variations to remain large even at long times.

To solve Eq. 2 for $\mathbf{w}$ in terms of $\widetilde{\mathrm{G}}$, we work in Fourier space and write the traceless part of $\widetilde{\mathrm{G}}$ in terms of the Q-dependent scalars $\widetilde{G}_{\parallel}$ and $\widetilde{G}_{\perp}$ (see also the SI):

$$\widetilde{G}_{ij} = \widetilde{G}_{ll}\frac{\delta_{ij}}{2} + (\widetilde{G}_{\parallel}\delta_{ik} - \widetilde{G}_{\perp}\epsilon_{ik})\left[\frac{2Q_kQ_j}{Q^2} - \delta_{kj}\right], \qquad [11]$$

where ϵ_{ij} is the Levi-Civita tensor. Plugging this into Eq. 2, we find the components of $\mathbf{w}$ longitudinal and transverse to $\mathbf{Q}$ in Fourier space:

$$w_k^{\parallel} = \frac{-i}{\lambda+2\mu}\left[(\lambda+\mu)\widetilde{G}_{ll} + 2\mu\ \widetilde{G}_{\parallel}\right]\frac{Q_k}{Q^2},$$
$$w_k^{\perp} = 2i\ \widetilde{G}_{\perp}\ \epsilon_{kl}\frac{Q_l}{Q^2}. \qquad [12]$$

And finally, we have the stress tensor:

$$\sigma_{ij} = 2(\lambda+\mu)\frac{\delta\rho}{\rho_0}\left[\frac{Q_iQ_j}{Q^2} - \delta_{ij}\right]. \qquad [13]$$

Strikingly, growth in an infinite system can thus only induce a nonzero stress when there is a non-vanishing density fluctuation $\delta\rho$ given by

$$\delta\rho = \rho_0\frac{\mu}{\lambda+2\mu}\left(\frac{\widetilde{G}_{ll} - 2\widetilde{G}_{\parallel}}{\bar{G}}\right). \qquad [14]$$

The noise ξ_{ij} in Eq. 4 now has three independent components. Keeping in mind the rotational invariance of ξ_{ij} (because we are perturbing around isotropic growth), we can choose ξ_{ll}, $\xi_{\parallel}$ and $\xi_{\perp}$ in the same vein as Eq. 11 as our statistically independent Gaussian random variables, where $\xi_{\parallel}$ and $\xi_{\perp}$ must have the same strength which can, however, differ from that of ξ_{ll}. As in the isotropic case, we require these random variables to be delta correlated in time but colored in space to avoid pathological behavior of the density-density correlators (see SI).

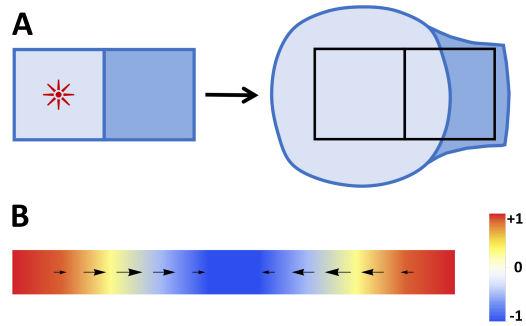

Fig. 2. (A) Independence of nearby clone areas. A localized region of growth (marked by the red star) at the center of the left clone (light blue) leads to an increase in the area of that clone, but it leaves the area of the adjacent clone (dark blue) unchanged even while distorting its shape. (B) Longitudinal soft mode. A sinusoidal growth leads to a strain field that fully compensates the growth field leaving the density unchanged. The arrows and their lengths indicate the direction and the magnitude of the deformation field $\mathbf{w}$. The color scale on the right gives the accumulated growth $\widetilde{G}$.

Substituting Eq. 13 for the stress into the growth dynamics Eq. 4, we find that the dynamics can be decomposed into three independent modes as (see SI)

$$\partial_t\,\delta\rho = -(k+k^{(d)})\delta\rho + \rho_0\frac{\mu}{\lambda+2\mu}\left(\xi_{ll} - 2\xi_{\parallel}\right), \qquad [15]$$
$$\partial_t\,Z_T = \xi_{\perp}, \qquad [16]$$
$$\partial_t\,Z_L = \xi_{ll} + 2\frac{k}{k^{(d)}}\xi_{\parallel}, \qquad [17]$$

where $Z_T = \widetilde{G}_{\perp}/\bar{G}$ and $Z_L = [\widetilde{G}_{ll} + 2(k/k^{(d)})\ \widetilde{G}_{\parallel}]/\bar{G}$ are the amplitudes respectively of transverse and longitudinal soft modes, which do not produce any stress and thus are allowed to grow diffusively. Before studying the density and clone statistics, we next consider these soft modes more carefully.

Soft Modes. As just shown, in two dimensions growth has two soft modes, Z_T and Z_L. They have the same physical origin: In each case, a nonuniform growth field $\widetilde{\mathrm{G}}$ induces a displacement field $\mathbf{w}$ that exactly cancels the effects of the growth, so that no mechanical stress results. This is illustrated for the longitudinal mode in Fig. 2B. Indeed, we have already seen (Eq. 13) that the stress is proportional to $\delta\rho$, so that only changes in density generate stress. Moreover, from Eq. 14 we can conclude that only growth perpendicular to $\mathbf{Q}$—that is, only the $\widetilde{G}_{22}$ component of $\widetilde{\mathrm{G}}$, in a basis in which $\mathbf{Q}$ points in the 1 direction—induces density changes; in all other cases, the system is able to deform to counteract the growth.

From Eqs. 16–17, one might imagine that the soft mode amplitudes grow without bound. This, however, turns out not to be the case. The reason is that the modes are defined at fixed Lagrangian wavevector $\mathbf{Q}$, whereas the noise terms $\xi_{\perp}$ and $\xi_{\parallel}$ have constant correlations in Eulerian space. As growth progresses, a given $\mathbf{Q}$ corresponds to longer and longer Eulerian lengthscales, leading to a decrease in the noise amplitude with time. As a result, as we show in the SI, the mean squared values of Z_L and Z_T remain bounded, even at long times.

Density-density Correlations. As in the isotropic case, we can calculate spatial and temporal density-density correlation functions for anisotropic growth. From Eq. 15, it is evident that the only differences between the two cases are the feedback

strength and the existence of a second noise term $\xi_\parallel$. The latter will only affect the pre-factors. We thus find that

$$\frac{1}{\rho_0^2}\left\langle \delta\rho(\mathbf{r},t)\delta\rho(\mathbf{0},t)\right\rangle_{t\to\infty} \sim \left(\frac{r}{a}\right)^{\frac{-2(k+k^{(d)})}{\gamma_0}}, \qquad [18]$$

and

$$\frac{1}{\rho_0^2}\left\langle \delta\rho(\mathbf{R},t)\delta\rho(\mathbf{R},t+\tau)\right\rangle_{t\to\infty} \sim e^{-(k+k^{(d)})\tau}, \qquad [19]$$

just as for isotropic growth, with prefactors of the same order.

Clone Statistics. In the isotropic case, where $\delta\rho$ was the only dynamical variable, mechanical feedback caused clone size and shape variations to decay in time relative to the average dilation. However, if we allow growth anisotropies, $\nabla.\mathbf{w}$ and $\mathbf{w}$, which are the relevant variables for clone properties (Eqs. 9 and 10), will depend not only on the density but also on the soft modes. In particular, from Eq. 12 we see that $\nabla.\mathbf{w}$ depends on $\delta\rho$ and Z_L while $\mathbf{w}$ depends on $\delta\rho$, Z_L and Z_T.

As mentioned above, the correlation functions for soft modes reach constant values at long times, whereas correlators that involve $\delta\rho$ decay exponentially in time. Thus $\langle\nabla.\mathbf{w}\ \nabla'.\mathbf{w}'\rangle$ and $\langle w_k w_j'\rangle$ will be dominated by soft modes at long times. We find for the clone size variations

$$\frac{\mathrm{Var}(A)}{\langle A\rangle^2} \sim \frac{1}{R_c^2} \qquad [20]$$

while for $n \geq 2$:

$$\frac{\left\langle |B_n|^2\right\rangle}{B_0^2} \sim \frac{1}{R_c^2}\frac{n}{n^2-1}, \qquad [21]$$

showing a slow $1/n$ decay. The pre-factors are $\mathcal{O}(1)$ if we assume $R_c \sim a$, i.e. that the clone is initially the size of a single cell.

According to Eq. 20, clone size variations scale with the size of the clone. We would get the same result for a population growing exponentially with a noise proportional to the square root of growth rate and no feedback (53). This means that the longitudinal soft mode overshadows the effect of feedback on density and thus, to study the clone size dynamics, one could naively ignore mechanical feedbacks and still get the same results.

Discussion

We have presented a simple model of noisy growth of elastic tissues with mechanical feedback. We found nontrivial behavior of experimentally accessible quantities including density-density correlation functions and clone size statistics.

We first showed that density correlations decay as a power law with distance. This behavior requires that fluctuations be correlated on some small length scale, whether because of the cutoff introduced by the finite cell size or because of Laplacian terms in the mechanical feedback. Using our result, it should be possible either to estimate the strength $c + c^{(d)}$ of the mechanical feedback, a quantity that has not been measured in growing tissues so far, or at least to put a lower bound on it. Somewhat counterintuitively, the sign of $c^{(d)}$ seems to be negative in some plant systems (43). We find that this does not destabilize growth as long as $c + c^{(d)} > 0$.

We then examined the statistics of clone growth. The properties of individual clones depend strongly on whether growth is isotropic or anisotropic. In the former case, mechanical feedback tends to prevent fluctuations on large scales, and the standard deviation in clone size becomes much smaller than the mean for large clones. This behavior changes dramatically in anisotropic growth because of the presence of soft modes that allow certain deformations to escape any negative feedback. As a consequence, in this case the standard deviation in clone area goes like the mean at long times, exactly as if the clone were an exponentially growing aggregate of randomly dividing cells that was not embedded in a surrounding tissue (53). Similarly, fluctuations in clone shape remain large when growth is anisotropic and soft modes dominate, but not when growth is restricted to be isotropic. Strikingly, we also find that the areas of different clones are always uncorrelated. This conclusion, together with the behavior of clone area fluctuations in the anisotropic case, implies that clones in elastic tissues have statistics that are no different from those in systems where mechanical feedback and crowding effects are completely absent.

We emphasize that the soft modes in our model are distinct from stress relaxation due to tissue fluidization (18). Whereas, in the latter case, stress decays exponentially in time, for soft modes it is identically zero. Our soft modes are related to the harmonic growth discussed in (20), which likewise does not generate any stress. Harmonic growth, however, occurs in finite tissues with isotropic growth and appropriate boundary conditions. Here, anisotropic soft modes are integral to the structure of the growth problem even in the absence of boundary effects.

Our model is the simplest that incorporates noise in the growth control problem. It neglects boundary effects, which can have important consequences. We have also ignored frictional forces. Friction always dominates for large enough growing tissues (54), but its effects can be small when growth is slow or when sources of drag are weak (as for plant tissues growing in air). Finally, by assuming a solid tissue, we neglected the possibility of cell flow and rearrangements (T1 transitions). Certainly, this assumption holds for plant cells (28, 29). In animal epithelia, there are cases where cell flows and T1's are significant (6). Nonetheless, in some developing tissues, like the *Drosophila* wing disc, cells do not appear to rearrange appreciably. For instance, clones of cells in the wing disc do not disperse (55, 56), Gibson et al. observed a lack of rearrangements in *ex vivo* wing discs of late 3rd instar larvae (57), and Farhadifar et al. showed using vertex model simulations that epithelial cell packings resemble a solid network rather than a soft, fluid-like one (58). Thus, it is reasonable to model the tissue as an elastic solid.

Our calculations also assume weak noise and hence small deformations. Importantly, this approximation is valid and self-consistent even in the presence of soft modes, because the soft mode amplitude is proportional to the noise strength and remains bounded at long times. Nonetheless, it would be of interest to explore what happens for stronger noise and larger deformations. Indeed, the statistical physics of noisy, nonequilibrium growth has a long and rich history (e.g. (59)), and from this perspective volumetric tissue growth represents an entirely new class of problems. Notably, we expect that the basic physics of the soft modes survives the transition to the nonlinear regime. In the general nonlinear case, it is convenient to characterize growth by a "target metric" (equal

to $G^T G$); if this metric lacks intrinsic curvature, it can always be compensated by a displacement field $\mathbf{w}$ and so will not generate any stresses (60).

The formalism presented here can also obviously be extended to include less generic effects, like inhomogeneous growth driven by morphogen gradients and chemical signaling, that are nonetheless crucial to many examples of morphogenesis and organ size control (22, 25). Our work is thus the first step towards more comprehensive models of specific biological systems.

ACKNOWLEDGMENTS. We are grateful to Alex Golden for helpful conversations. This work was supported in part by National Science Foundation grant DMR-1056456, by the Margaret and Herman Sokol Faculty Awards, and by the NSF Graduate Research Fellowship Program under grant DGE-1256260.

1. Milán M, Campuzano S, García-Bellido A (1996) Cell cycling and patterned cell proliferation in the wing primordium of drosophila. *Proc Natl Acad Sci U S A* 93(2):640–645.
2. Klein AM, Doupe DP, Jones PH, Simons BD (2007) Kinetics of cell division in epidermal maintenance. *Phys Rev E Stat Nonlin Soft Matter Phys* 76(2 Pt 1):021910.
3. Meyer HM, Roeder AHK (2014) Stochasticity in plant cellular growth and patterning. *Front Plant Sci* 5:420.
4. Klein AM, Simons BD (2011) Universal patterns of stem cell fate in cycling adult tissues. *Development* 138(15):3103–11.
5. de Navascués J, et al. (2012) Drosophila midgut homeostasis involves neutral competition between symmetrically dividing intestinal stem cells. *EMBO J* 31(11):2473–2485.
6. Rulands S, et al. (2018) Universality of clone dynamics during tissue development. *Nat Phys* 14(5):469–474.
7. Heemskerk I, Lecuit T, LeGoff L (2014) Dynamic clonal analysis based on chronic in vivo imaging allows multiscale quantification of growth in the drosophila wing disc. *Development* 141(11):2339–48.
8. Pan Y, Heemskerk I, Ibar C, Shraiman BI, Irvine KD (2016) Differential growth triggers mechanical feedback that elevates hippo signaling. *Proc Natl Acad Sci U S A* 113(45):E6974–E6983.
9. Greulich P, Simons BD (2016) Dynamic heterogeneity as a strategy of stem cell self-renewal. *Proc Natl Acad Sci U S A* 113(27):7509–7514.
10. Tsugawa S, et al. (2017) Clones of cells switch from reduction to enhancement of size variability in arabidopsis sepals. *Development* 144(23):4398–4405.
11. Puliafito A, et al. (2012) Collective and single cell behavior in epithelial contact inhibition. *Proc Natl Acad Sci U S A* 109(3):739–44.
12. Streichan SJ, Hoerner CR, Schneidt T, Holzer D, Hufnagel L (2014) Spatial constraints control cell proliferation in tissues. *Proc Natl Acad Sci U S A* 111(15):5586–91.
13. Zehnder SM, Suaris M, Bellaire MM, Angelini TE (2015) Cell volume fluctuations in mdck monolayers. *Biophys J* 108(2):247–50.
14. Zehnder SM, et al. (2015) Multicellular density fluctuations in epithelial monolayers. *Phys Rev E Stat Nonlin Soft Matter Phys* 92(3):032729.
15. Puliafito A, Primo L, Celani A (2017) Cell-size distribution in epithelial tissue formation and homeostasis. *J R Soc Interface* 14(128):20170032.
16. Chen DY, Aw WY, Devenport D, Torquato S (2016) Structural characterization and statistical-mechanical model of epidermal patterns. *Biophys J* 111(11):2534–2545.
17. Leamy LJ, Klingenberg CP (2005) The genetics and evolution of fluctuating asymmetry. *Annual Review of Ecology, Evolution, and Systematics* 36(1):1–21.
18. Ranft J, et al. (2010) Fluidization of tissues by cell division and apoptosis. *Proc Natl Acad Sci U S A* 107(49):20863–20868.
19. Shraiman BI (2005) Mechanical feedback as a possible regulator of tissue growth. *Proc Natl Acad Sci U S A* 102(9):3318–23.
20. Irvine KD, Shraiman BI (2017) Mechanical control of growth: ideas, facts and challenges. *Development* 144(23):4238–4248.
21. Hufnagel L, Teleman AA, Rouault H, Cohen SM, Shraiman BI (2007) On the mechanism of wing size determination in fly development. *Proc Natl Acad Sci U S A* 104(10):3835–40.
22. Aegerter-Wilmsen T, Aegerter CM, Hafen E, Basler K (2007) Model for the regulation of size in the wing imaginal disc of drosophila. *Mech Dev* 124(4):318–26.
23. Ramasubramanian A, Taber LA (2008) Computational modeling of morphogenesis regulated by mechanical feedback. *Biomech Model Mechanobiol* 7(2):77–91.
24. Aegerter-Wilmsen T, et al. (2010) Exploring the effects of mechanical feedback on epithelial topology. *Development* 137(3):499–506.
25. Aegerter-Wilmsen T, et al. (2012) Integrating force-sensing and signaling pathways in a model for the regulation of wing imaginal disc size. *Development* 139(17):3221–31.
26. Alim K, Hamant O, Boudaoud A (2012) Regulatory role of cell division rules on tissue growth heterogeneity. *Front Plant Sci* 3:174.
27. Hannezo E, Prost J, Joanny JF (2014) Growth, homeostatic regulation and stem cell dynamics in tissues. *J R Soc Interface* 11(93):20130895.
28. Hervieux N, et al. (2016) A mechanical feedback restricts sepal growth and shape in arabidopsis. *Curr Biol* 26(8):1019–1028.
29. Hervieux N, et al. (2017) Mechanical shielding of rapidly growing cells buffers growth heterogeneity and contributes to organ shape reproducibility. *Curr Biol* 27(22):3468–3479.e4.
30. Kursawe J, Brodskiy PA, Zartman JJ, Baker RE, Fletcher AG (2015) Capabilities and limitations of tissue size control through passive mechanical forces. *PloS Comput Biol* 11(12):26.
31. Lee SW, Morishita Y (2017) Possible roles of mechanical cell elimination intrinsic to growing tissues from the perspective of tissue growth efficiency and homeostasis. *PLoS Comput Biol* 13(7):e1005651.
32. Buchmann A, Alber M, Zartman JJ (2014) Sizing it up: The mechanical feedback hypothesis of organ growth regulation. *Semin Cell Dev Biol* 35:73–81.
33. Ma M, Cao X, Dai J, Pastor-Pareja JC (2017) Basement membrane manipulation in drosophila wing discs affects dpp retention but not growth mechanoregulation. *Dev Cell* 42(1):97–106 e4.
34. Schluck T, Nienhaus U, Aegerter-Wilmsen T, Aegerter CM (2013) Mechanical control of organ size in the development of the drosophila wing disc. *PLOS ONE* 8(10):e76171.
35. Wyatt TPJ, et al. (2015) Emergence of homeostatic epithelial packing and stress dissipation through divisions oriented along the long cell axis. *Proc Natl Acad Sci U S A* 112(18):5726–31.
36. Gudipaty SA, et al. (2017) Mechanical stretch triggers rapid epithelial cell division through piezo1. *Nature* 543(7643):118–121.
37. Legoff L, Rouault H, Lecuit T (2013) A global pattern of mechanical stress polarizes cell divisions and cell shape in the growing drosophila wing disc. *Development* 140(19):4051–9.
38. Mao Y, et al. (2013) Differential proliferation rates generate patterns of mechanical tension that orient tissue growth. *EMBO J* 32(21):2790–803.
39. LeGoff L, Lecuit T (2016) Mechanical forces and growth in animal tissues. *Cold Spring Harb Perspect Biol* 8(3):a019232.
40. Marinari E, et al. (2012) Live-cell delamination counterbalances epithelial growth to limit tissue overcrowding. *Nature* 484(7395):542–5.
41. Wagstaff L, et al. (2016) Mechanical cell competition kills cells via induction of lethal p53 levels. *Nat Commun* 7:11373.
42. Levayer R, Dupont C, Moreno E (2016) Tissue crowding induces caspase-dependent competition for space. *Curr Biol* 26(5):670–677.
43. Uyttewaal M, et al. (2012) Mechanical stress acts via katanin to amplify differences in growth rate between adjacent cells in arabidopsis. *Cell* 149(2):439–451.
44. Delarue M, Joanny JF, Jülicher F, Prost J (2014) Stress distributions and cell flows in a growing cell aggregate. *Interface Focus* 4(6):20140033.
45. Delarue M, et al. (2014) Compressive stress inhibits proliferation in tumor spheroids through a volume limitation. *Biophys J* 107(8):1821–1828.
46. Taloni A, Ben Amar M, Zapperi S, La Porta AMC (2015) The role of pressure in cancer growth. *The European Physical Journal Plus* 130(11):1–10.
47. Winkle JJ, Igoshin OA, Bennett MR, Josic K, Ott W (2017) Modeling mechanical interactions in growing populations of rod-shaped bacteria. *Phys Biol* 14(5):055001.
48. Delarue M, et al. (2016) Self-driven jamming in growing microbial populations. *Nat Phys* 12(8):762–766.
49. Goriely A (2017) *The Mathematics and Mechanics of Biological Growth*. (Springer New York).
50. Landau LD, Lifshitz EM (1986) *Theory of elasticity*. (Butterworth-Heinemann).
51. Nowacki W (1986) *Thermoelasticity*. (Pergamon Press ; PWN-Polish Scientific Publishers).
52. Liddle A, Lyth D (2000) *Cosmological Inflation and Large-Scale Structure*. (Cambridge University Press).
53. Van Kampen N (2011) *Stochastic Processes in Physics and Chemistry*, North-Holland Personal Library. (Elsevier Science).
54. Blanch-Mercader C, Casademunt J, Joanny JF (2014) Morphology and growth of polarized tissues. *The European Physical Journal E* 37(5):1–11.
55. Garcia-Bellido A, Ripoll P, Morata G (1973) Developmental compartmentalisation of the wing disk of drosophila. *Nat New Biol* 245(147):251–3.
56. Garcia-Bellido A, Ripoll P, Morata G (1976) Developmental compartmentalization in the dorsal mesothoracic disc of drosophila. *Dev Biol* 48(1):132–147.
57. Gibson MC, Patel AB, Nagpal R, Perrimon N (2006) The emergence of geometric order in proliferating metazoan epithelia. *Nature* 442(7106):1038–41.
58. Farhadifar R, Röper JC, Aigouy B, Eaton S, Jülicher F (2007) The influence of cell mechanics, cell-cell interactions, and proliferation on epithelial packing. *Curr Biol* 17(24):2095–2104.
59. Kardar M, Parisi G, Zhang YC (1986) Dynamic scaling of growing interfaces. *Phys Rev Lett* 56(9):889–892.
60. Golden AD (2018) Feedback models in biological physics, Phd thesis. University of Michigan.